SE(R)RS excitation profile of free-base 5,10,15,20-tetrakis(1-methyl-4-pyridyl)porphyrin on immobilized gold nanoparticles

Natália Hajduková-Šmídová[1], Marek Procházka[1,], Minoru Osada[2]*
[1]Institute of Physics, Faculty of Mathematics and Physics, Charles University, Prague, 121 16 Czech Republic
[2]International Center for Materials Nanoarchitectonics (MANA), National Institute for Materials Science (NIMS), Tsukuba, Ibaraki 305-0044, Japan

[*]Corresponding author: tel. + 420 221 911 474, fax + 420 224 922 797,
e-mail: prochaz@karlov.mff.cuni.cz

Abstract
Surface-enhanced (resonance) Raman scattering - SE(R)RS - excitation profile (dependence of SE(R)RS intensity on excitation wavelength) is a key point for optimizing of electromagnetic enhancement of particular SE(R)RS system. In this paper, we measured SE(R)RS excitation profile of free-base 5,10,15,20-tetrakis(1-methyl-4-pyridyl) porphyrin (TMPyP) on immobilized Au nanoparticles using confocal Raman microspectrometer with six excitation wavelengths (457.9, 488.0, 514.5, 530.9, 568.2 and 647.1 nm). Au colloidal nanoparticles were immobilized to a glass slide surface *via* a self-assembled monolayer of 3-aminopropyltrimethoxysilane. SE(R)RS excitation profile is correlated with the corresponding surface plasmon extinction (SPE) spectrum of immobilized Au nanoparticles although the maximum of SE(R)RS intensity is slightly shifted from maximum of SPE. In our case of resonant molecule, SE(R)RS enhancement is coupled with molecular resonance enhancement and SE(R)RS excitation profile for particular vibrational mode depends on its TMPyP molecular resonance contribution. SE(R)RS excitation profile shows that maximal SE(R)RS intensity is obtained for 568.2 nm excitation that provides limit of detection (LOD) of TMPyP 2×10^{-8} M in soaking solution.

Keywords: SERS, SERRS, excitation profile, gold nanoparticles, porphyrin

1. Introduction

Surface-enhanced Raman scattering (SERS) spectroscopy is an extremely sensitive analytical technique providing a giant signal enhancement (up to 10^6-fold) of Raman scattering (RS) for molecules adsorbed onto a suitable nanostructured metal surface [1]. Principal SERS enhancement mechanism (known as electromagnetic) is related to excitation of localized surface plasmon resonance (LSPR) in the metal nanostructures [2]. The most commonly used SERS-active metals are silver and gold because both have LSPR frequencies in the visible region. The largest SERS enhancement is expected when the wavelength of excitation laser and/or of Stokes-shifted Raman light is close to the resonance wavelength [2]. Resonance wavelength can be extracted from surface plasmon extinction (SPE) spectrum of the employed SERS-active metal substrate in some cases. The connection between SPE and the electromagnetic SERS enhancement is, however, indirect in general. For example, in the case of the highly aggregated colloidal solutions when SERS signal comes from a small number of highly enhanced sites (hot-spots), the largest SERS efficiency is out of SPE maximum. This is due to the different spatial localization of collective resonances and their different spatial averaging properties [2, 3]. Moreover, isolated Ag nanoarrays show red and blue shift of the maximum SERS signal with respect to the maximum of LSPR of bare and adsorbate-covered nanoarray, respectively [4]. Thus, SERS

excitation profile (dependence of SERS intensity on excitation wavelength) is in many cases a key point for optimizing of experimental conditions of particular SERS measurement.

SERS as an extremely sensitive detection technique for small quantities of molecules (even for single molecule detection) provides many bioanalytical and biomedical applications [5]. Porphyrins and their derivatives are a good example of highly SERS-active biomolecules [6-13]. Biological importance of these molecules includes applications in photodynamic therapy of cancer, antiviral treatments, molecular biology, specific sensing of DNA sequences, selective cleavage of nucleic acids and transport of oligonucleotides into the cells [14]. Molecular resonance of porphyrins in visible region causes an efficient fluorescence, process competitive to resonance Raman scattering (RRS), which complicates Raman measurement. SERS spectroscopy provides a unique possibility how to measure Raman spectra of highly fluorescent porphyrins due to efficient fluorescence quenching. In the case when excitation wavelength falls simultaneously close to molecular resonance of porphyrin as well as to LSPR of SERS-active substrate, SERS intensity is also affected by molecular resonance enhancement and this phenomenon is called surface-enhanced resonance Raman scattering (SERRS).

In this paper, we measured SE(R)RS excitation profile of free-base 5,10,15,20-tetrakis(1-methyl-4-pyridyl) porphyrin (TMPyP, see chemical structure in Fig. 1) adsorbed on immobilized Au nanoparticles using confocal Raman microspectrometer with six excitation wavelengths (457.9, 488, 514.5, 530.9, 568.2 and 647.1 nm). Au colloidal nanoparticles were immobilized to a glass slide surface *via* a self-assembled monolayer of 3-aminopropyltrimethoxysilane (APTMS) [15-17]. The main advantage of this method is that Au nanoparticles are not strongly aggregated and Au surface is stable and gives reproducible SERS signal [17]. Moreover, free-base porphyrin molecules are not metalated [11, 12] (process known for free-base porphyrins adsorbed on bare Ag colloidal nanoparticles [8-10]) by Au atoms from the substrate and thus we can obtain SE(R)RS excitation profile from free-base unperturbed porphyrin species. We discuss relation between SE(R)RS intensity and SPE spectrum of the system and compare it with (R)RS profile of the porphyrin.

2. Experimental

Deionized water of a specific resistance of 18 MΩcm was used for all preparations. H_2SO_4 (98%), H_2O_2 (30%), HCl (36%) and HNO_3 (69%) were obtained from PENTA. $HAuCl_4$, sodium citrate, methanol (99.8%), 3-aminopropyltrimethoxysilane (APTMS, 97%) and 5,10,15,20-tetrakis(1-methyl-4-pyridyl) porphyrin (TMPyP) were purchased from Sigma–Aldrich. All glassware was cleaned using “piranha” solution (4 parts H_2SO_4, 1 part H_2O_2) to remove organics and then aqua regia (3 parts HCl, 1 part HNO_3) for removal of metals.

Au colloidal nanoparticles were prepared by reduction of $HAuCl_4$ by sodium citrate: 250 ml of 1 mM solution of $HAuCl_4$ was brought to a boil and then 25 ml of 38.8 mM solution of sodium citrate was added. Boiling continued for 15 minutes and then the solution was left to cool.

Clean glass slides (1 cm × 2 cm strips) were derivatized in 10% of APTMS in methanol for 30 min. After the silanization, substrates were rinsed several times with methanol and then with water to remove any physisorbed organosilane, which could cause aggregation of colloidal particles in suspension during next step. Each silanized glass plate was dipped in vertical position (metal surface is thus formed on both sides of the glass slide) into colloidal suspension for 3–4 h. Then the plates were rinsed with water. Substrates were after left to dry at 100 °C for 10 min. Preparation of Au surfaces is described in detail in our previous paper [17].

TMPyP was dissolved in water. Dependences of the SE(R)RS spectra on the soaking time were measured as follows: Au substrate was placed for an appropriate period in contact with the porphyrin solution and then was rinsed by deionized water and SE(R)RS spectrum was measured. The substrate was then placed again in the same porphyrin solution for additional time, rinsed by deionized water, and the SE(R)RS spectrum then was measured.

The soaking–rinsing–measuring cycles were repeated gradually and the total time of soaking was counted. The concentration dependence of the SE(R)RS spectra was measured in the same way, but the soaking time was fixed and the porphyrin concentration was gradually increased. For SE(R)RS excitation profile measurements, Au substrate was placed into the porphyrin solution for definite time, then it was rinsed by deionized water and SE(R)RS spectra were measured.

(R)RS and SE(R)RS spectra were recorded at room temperature with a confocal micro-Raman spectrometer (Horiba-Jobin Yvon, T64000) in backscattering geometry using six lines (457.9, 488.0, 514.5, 530.9, 568.2 and 647.1 nm) of an Ar^+/Kr^+ mixed gas laser (Spectra Physics 2060) with the power of 0.06, 0.2, 0.2, 0.2, 0.07 and 0.2 mW at the sample for particular line, respectively. Excitation light was collected by a long-working-distance lens (Olympus, 90x, NA: 0.75) to achieve about 1 μm diameter of the spot at the surface. Scattered radiation was detected with a liquid-nitrogen-cooled charge-couple device (CCD) detector (Horiba-Jobin Yvon, Symphony, 1024 x 256 pixels) coupled to a Horiba-Jobin Yvon T64000 spectrograph with a 600 grooves/mm grating. Accumulation time was 3×15 s and spectra were normalized to Raman signal of silicon. Surface plasmon extinction (SPE) spectra of Au substrates were recorded on a Hitachi U-4000 ultraviolet-visible absorption spectrometer. Scanning electron microscopy (SEM) images were obtained by using a Hitachi S5000 device. Atomic force microscopy (AFM) images were obtained by using a SII Nanotech SPA400.

3. Results and Discussion

3.1. Characterization of Au surfaces

Prepared Au surfaces were characterized from the point of view of their optical response and surface morphology. Typical SPE spectra of the parent Au colloidal solution and immobilized Au colloidal nanoparticles on glass are shown in Fig. 2. Au substrates are grey-violet with a broad SPE band between 500 and 600 nm (curve B) close to this of parent colloid (see curve A) and thus corresponding to isolated and/or only slightly interacting gold nanoparticles. AFM and SEM images of Au substrates (Fig. 3) demonstrate a compact coverage of glass by Au nanoparticles of diameters varying from ~ 30 to 100 nm and by small aggregates. Scanning of the whole surface and comparing several substrates indicate that our Au substrates are uniform and the preparation is highly reproducible.

3.2. Optimization of conditions for SERS measurements of TMPyP

First Raman experiments were focused on obtaining of optimal conditions, i.e. optimal adsorption (soaking) time and TMPyP concentration on Au substrates using common 514.5 nm excitation wavelength. SE(R)RS intensity was determined by an integral intensity of the strongest TMPyP band at ~ 1550 cm^{-1} and normalized (maximal intensity = 1) for all cases. Time evolution of the TMPyP adsorption was monitored *via* SERRS spectra measured for different soaking times (from 1 to 60 min) when TMPyP soaking concentration was fixed (Fig. 4, left). In the case of the lowest TMPyP concentration (1×10^{-6} M) the SERRS signal significantly increases with soaking time. For higher concentrations, the soaking time of 25–30 min seems to be optimal showing clear saturation of SERRS signal for longer times.

Dependences of the SERRS spectra on TMPyP concentration were measured in 1×10^{-7} - 3×10^{-5} M range for 15, 20, 25 and 30 min soaking times (Fig. 4, right). In all cases, the SERRS signal increases rapidly up to ~ 1×10^{-5} M concentration and then is saturated. This level should correspond to a covering limit of the porphyrin molecules on the Au surface. Thus, optimal conditions for SE(R)RS study of TMPyP on our Au substrates are $1x10^{-5}$ M TMPyP soaking concentration and 30 min soaking time.

3.3. (R)RS and SE(R)RS excitation profiles of TMPyP

(R)RS excitation profile was measured from a drop of TMPyP of $1x10^{-3}$ M concentration dried on a pure glass. Spectra obtained for yellow and red excitation line show fluorescence

background which is stronger for higher wavelengths and makes obtaining of RRS spectrum of TMPyP difficult. In the case of 647.1 nm excitation line we were not able to extract RRS spectrum of TMPyP from fluorescence background. SE(R)RS excitation profile was measured under optimized conditions ($1x10^{-5}$ M TMPyP soaking concentration and 30 min soaking time) and six excitation wavelengths.

Baseline-corrected (R)RS and SE(R)RS spectra of TMPyP measured using particular excitation wavelength are compared in Fig. 5. All SE(R)RS spectra contain typical bands of free-base TMPyP at ~ 331, 1334+1358, 1552 cm^{-1} [8] proving that TMPyP is not metalated by Au after adsorption on Au substrate [11, 12]. Observed (R)RS and SE(R)RS bands are listed in Table 1 together with their tentative assignment taken from references 18-22. Comparing SE(R)RS and (R)RS spectra measured for particular excitation, slight intensity changes caused by adsorption of TMPyP on Au surface can be seen. The 1634, 1292, 1245, 1215 and 402 cm^{-1} bands seem to be more enhanced than the other ones indicating mostly flat orientation of the porphyrin core on the surface as well as some tilt of the external N-methylpyridyl groups interacting with Au surface [20, 22]. Moderate enhancement of 1332 and 1552 cm^{-1} bands as well as appearance of new bands at 1498 and 715 cm^{-1} in SE(R)RS spectra correspond to deformation of the porphyrin macrocycle during adsorption. Both (R)RS and SE(R)RS spectra show also significant spectral changes as a function of excitation wavelength (will be discussed below).

(R)RS excitation profile of TMPyP is plotted in the left part of Fig. 6 together with electronic absorption spectrum of TMPyP solution. SPE spectrum of Au substrate/TMPyP and corresponding SE(R)RS excitation profile of TMPyP are shown in Fig. 6, right. In this case, (R)RS and/or SE(R)RS intensities were determined as integral intensity of whole spectra in 300-1700 cm^{-1} region. (R)RS excitation profile shows that the highest intensity is obtained for 457.9 nm excitation (falling into the absorption Soret band of TMPyP at 424 nm) while substantially lower intensity is observed for other excitations (falling into the absorption Q-bands of TMPyP). It is in agreement with the fact that RRS of porphyrins is intense when excited in the Soret band and that spectra within the Q-bands are normally weaker [20, 22].

SE(R)RS excitation profile is correlated with the corresponding SPE extinction spectrum (LSPR): the highest SE(R)RS intensity is obtained for 568.2 nm excitation line. On the other hand, the maximum of SE(R)RS intensity (~570 nm) is slightly shifted from maximum of SPE (~545 nm). SE(R)RS excitation profile of TMPyP for particular spectral bands is shown in Fig. 7 (normalized to maximal intensity). There are three groups of spectral bands with different excitation profile: (i) 331, 1245, 1332, 1552 cm^{-1} with excitation profile correlated with SPE, maximum at ~ 570 nm (red shift) (ii) 1000, 1215, 1635 cm^{-1} with excitation profile correlated with SPE, maximum at ~ 530 nm (blue shift) and (iii) 965 cm^{-1} with excitation profile correlated with (R)RS excitation profile of TMPyP. On the basis of vibrational assignment (see Table 1) one can see that the spectral bands of particular group with the same behavior (i-iii) include the same vibrational modes: (i) stretching and bending deformations of porphyrin core, all very sensitive to metalation and/or stacking [8, 9], (ii) stretching and bending deformations of N-methylpyridyl group. The 965 cm^{-1} band (iii) is assigned to stretching deformation of C_α-C_β or C_α-C_m . We suggest that differences in SE(R)RS excitation profiles for three groups of vibrational modes is caused by different contribution of molecular resonance of particular vibrational mode of TMPyP for particular excitation wavelength.

3.4. SE(R)RS detection limit of TMPyP

SE(R)RS excitation profile shows that the best SERS enhancement is obtained for 568.2 nm excitation. Thus, we used this excitation to determine the limit of detection (LOD) of TMPyP on our Au substrates. SERS spectra of TMPyP of soaking concentrations between 1×10^{-5} M and $\sim5\times10^{-8}$ M are shown in Fig. 8. The LOD was determined by extrapolation to the concentration for which the SERS intensity exceeds the triple of the blank signal standard deviation [12, 23]. The LOD of TMPyP on our Au substrates determined in this way is 2×10^{-8} M soaking solution for 568.2 nm excitation.

4. Conclusions

Au colloidal nanoparticles have been immobilized on glass *via* a self-assembled monolayer of 3-aminopropyltrimethoxysilane (APTMS). The main advantage of this method is that such Au substrates are stable and give reproducible SERS signal. 5,10,15,20-tetrakis(1-methyl-4-pyridyl) porphyrin (TMPyP) has been adsorbed on the Au substrates and experimental conditions for SE(R)RS have been optimized. The optimal conditions for SE(R)RS study of TMPyP are $1x10^{-5}$ M TMPyP soaking concentration and 30 min soaking time. SE(R)RS excitation profile of TMPyP has been measured under these optimized conditions and six excitation wavelengths (457.9, 488, 514.5, 530.9, 568.2 and 647.1 nm). The free-base porphyrin molecules are not metalated by Au atoms from the substrate and thus we obtained SE(R)RS excitation profile from free-base unperturbed porphyrin species. SE(R)RS excitation profile is correlated with the surface plasmon extinction (SPE) spectrum of immobilized Au nanoparticles but SE(R)RS enhancement is coupled with molecular resonance enhancement of TMPyP. SE(R)RS excitation profile peak position for particular vibrational mode is slightly shifted from SPE maximum position depending of its molecular resonance contribution (red or blue shift). Vibrational mode at 965 cm^{-1} fits (R)RS excitation profile of TMPyP but not SPE spectrum of Au surface. SE(R)RS excitation profile shows that the best SERS enhancement is obtained for 568.2 nm excitation that provides limit of detection (LOD) of TMPyP 2×10^{-8} M in soaking solution.

Acknowledgments
This work was supported by the Czech Science Foundation (P205/12/G118) and NIMS Junior Researcher Fellowship under the "Charles University – NIMS Joint Graduate School Program". We thank Břetislav Šmíd from Department of Surface and Plasma Science, Faculty of Mathematics and Physics, Charles University for carry out SEM images of Au surfaces in NIMS.

Table 1. Observed (R)RS and SE(R)RS bands of TMPyP and their tentative assignments.

(R)RS (cm^{-1}) exc. 457.9 nm	**SE(R)RS (cm^{-1}) exc. 568.2 nm**	**band assignment**
1635 (m)	1635 (w)	δ(pyr) [18,19,21,22]
1552 (s)	1552 (s)	$\nu(C_\beta - C_\beta)$ [18,19,21,22]
	1498 (w)	$\nu(C_\beta - C_\beta)$ [19]
1448 (w)	1451 (s)	$\nu(C_\alpha - C_m) + \nu(C_\alpha - C_\beta)$ [18,19] or pyr, ν(C-C) [22]
1357 (w)	1332+1358 (m)	$\nu(C_\alpha - N)$ [18,19,21,22]
1292 (m)	1290 (w)	δ(pyr) [18,22]
1245 (m)	1245 (s)	$\delta(C_m$-pyr) [18,19,21,22]
1215 (m)	1214 (w)	δ(pyr) [18,19,22]
	1138 (w)	$\nu(C_\alpha - C_\beta)$ [22]
1098 (w)	1100 (w)	$\delta(C_\beta$-H) [21,22]
1000 (s)	1000 (w)	ν(pyr) [18,22]
965 (m)	965 (w)	$\nu(C_\alpha - C_\beta)$ [19] or $\nu(C_\alpha - C_m)$ [22]
793 (w)	805 (w)	pyr, ν(C-C)+ $\nu(N^+$-$CH_3)$ [19,21]
712 (w)	715 (w)	δ(pyr) [21]
665 (w)	666 (w)	δ(pyr)+ $\delta(C$-N^+-$CH_3)$ [19,21]
403 (w)	402 (w)	γ(por) [19,22]
331 (m)	331 (w)	δ(por) [18, 22]

Abbreviations: s - strong, m - medium, w- weak, por - porphyrin core, pyr - N-methylpyridyl group, ν - stretching deformation, δ - bending deformation, γ - out-of-plane folding. Vibrational assignments taken from ref. 18, 19, 21, 22.

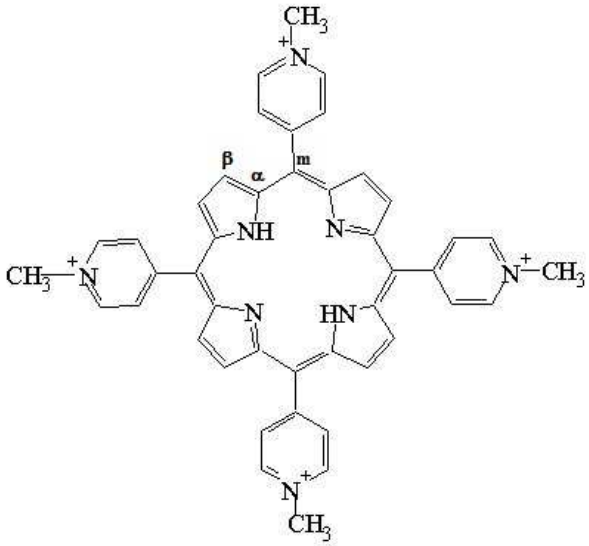

Figure 1. Chemical structure of 5,10,15,20-tetrakis(1-methyl-4-pyridyl) porphyrin (TMPyP).

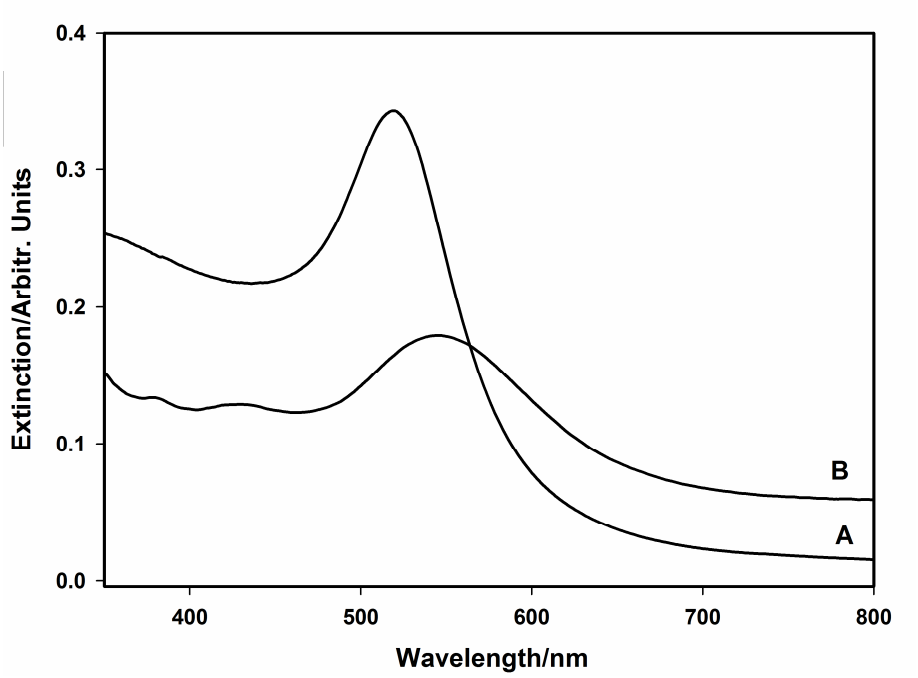

Figure 2. Typical SPE spectra of the parent Au colloid (A) and Au substrate (B).

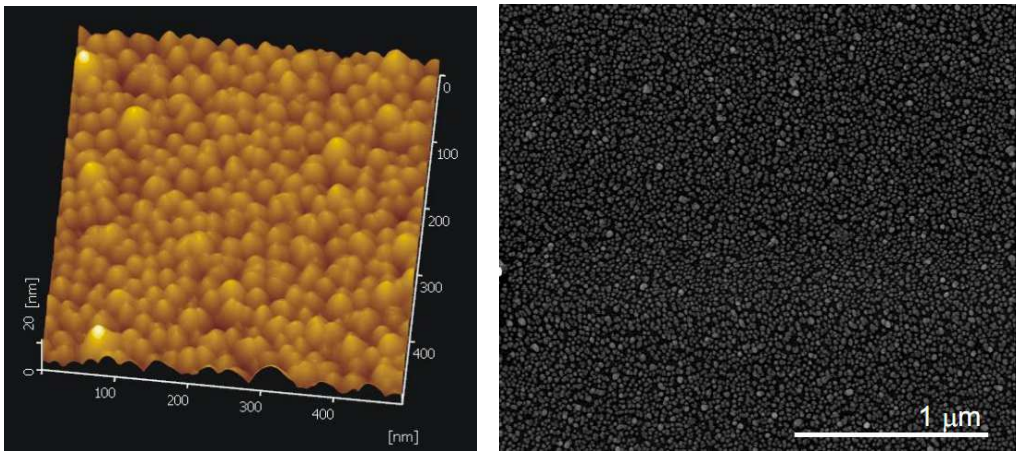

Figure 3. Typical AFM (left) and SEM (right) images of Au substrates.

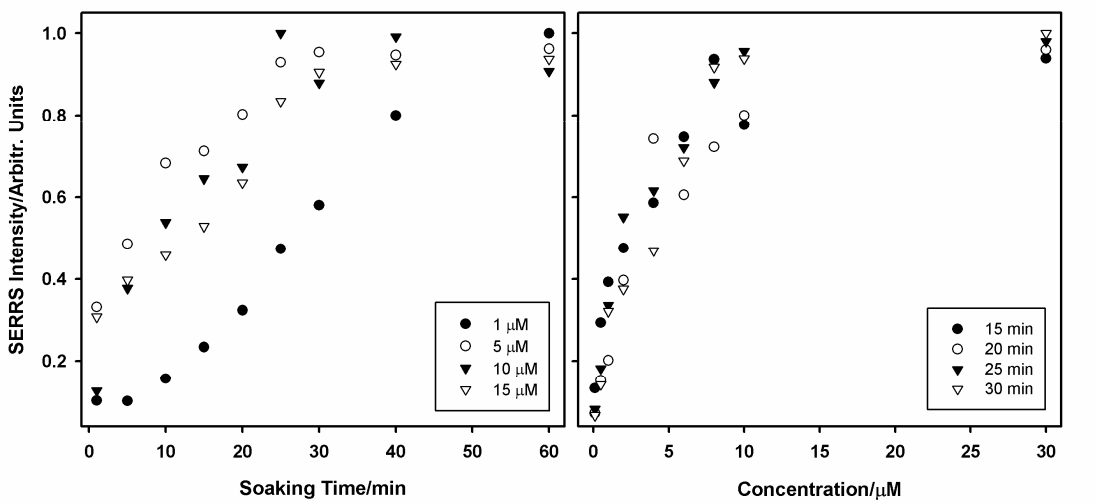

Figure 4. Optimization of SERRS measurements: dependences of TMPyP SERRS intensity on soaking time (left) and TMPyP concentration (right) measured using 514.5 nm excitation line.

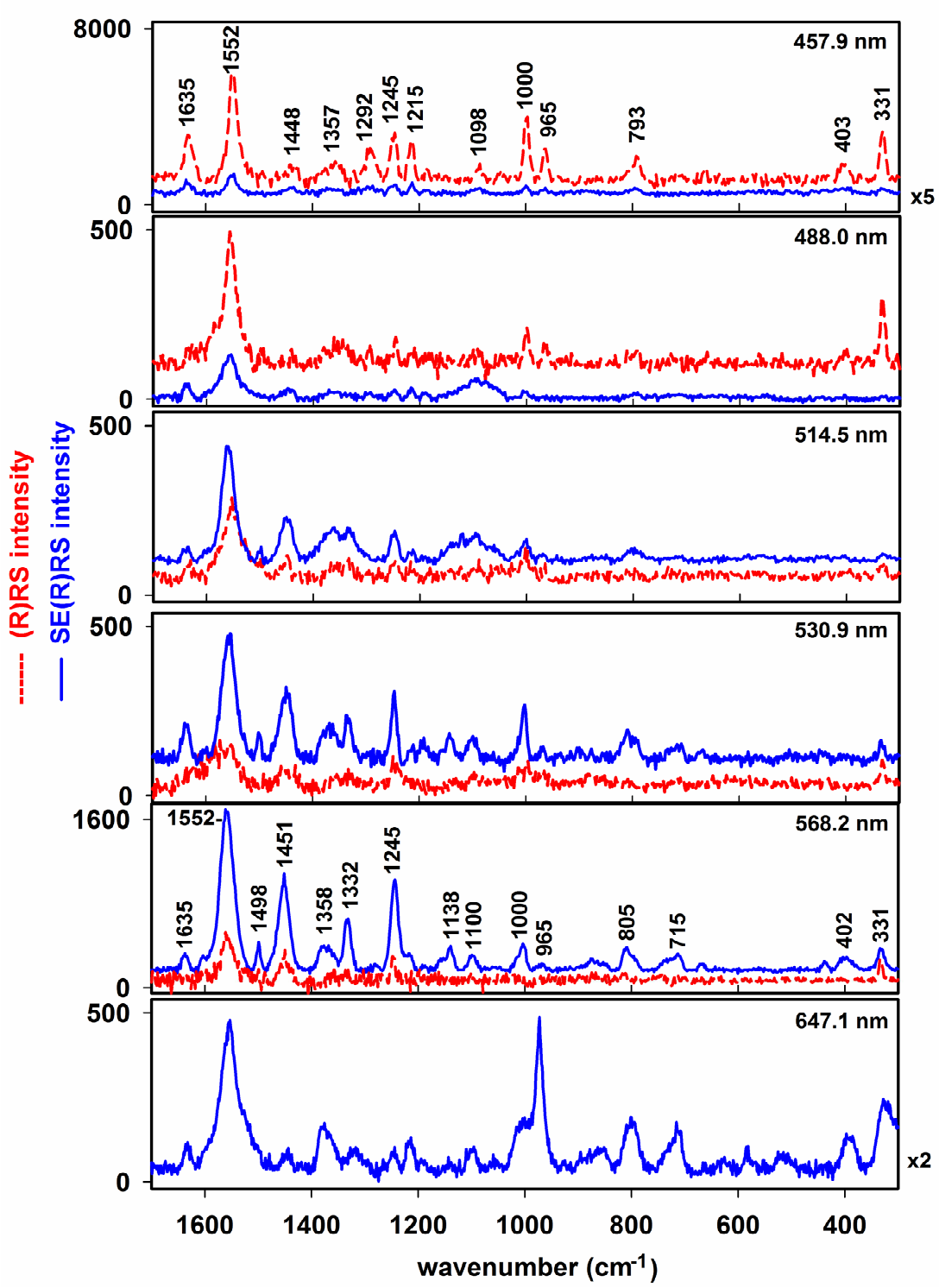

Figure 5. Comparison of (R)RS and SE(R)RS spectra of TMPyP measured using different excitation wavelengths. All spectra are baseline-corrected.

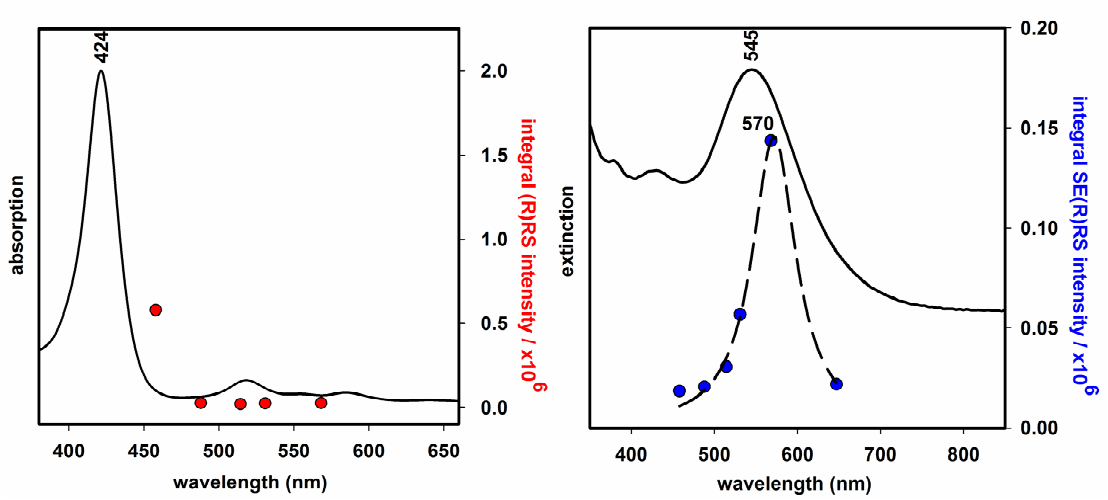

Figure 6. Left: (R)RS excitation profile of TMPyP and electronic absorption spectrum of TMPyP solution. Right: SPE spectrum of Au substrate/TMPyP and corresponding SE(R)RS excitation profile of TMPyP.

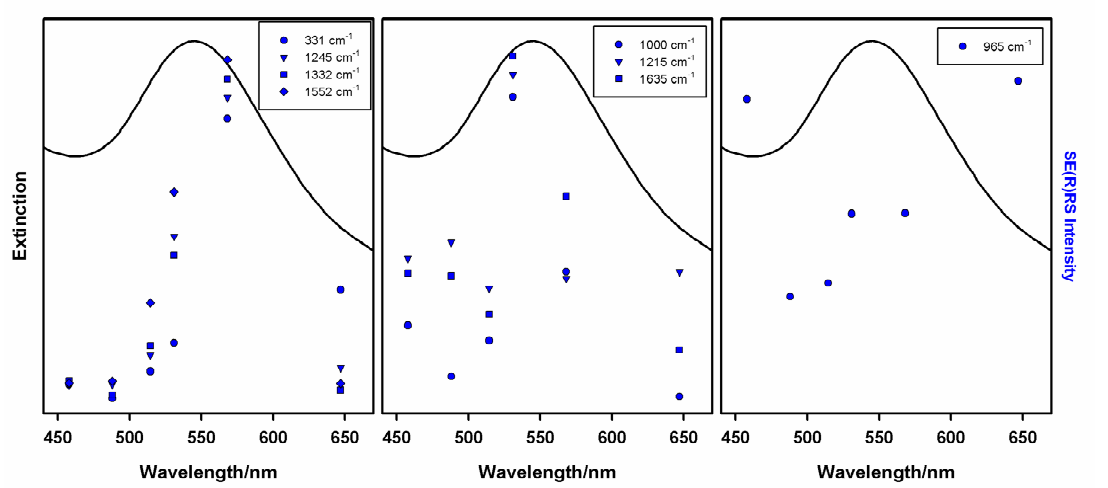

Figure 7. SE(R)RS excitation profile of TMPyP for particular vibrational modes.

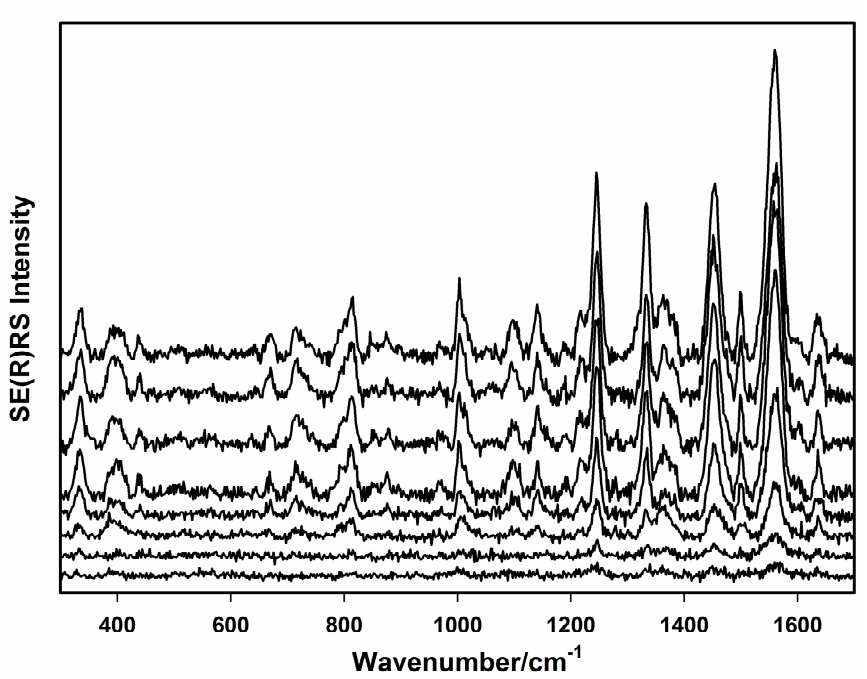

Figure 8. Concentration dependence of SERS spectra of TMPyP measured using 568.2 nm excitation line. Soaking concentration from top to bottom: 1×10^{-5}, 6×10^{-6}, 3×10^{-6}, 1×10^{-6}, 6×10^{-7}, 3×10^{-7}, 1×10^{-7}, 5×10^{-8} M. All spectra are baseline-corrected.

References

[1] M. Fleischmann, P.J. Hendra, A.J. McQuillan, Chem. Phys. Lett. 26 (1974) 163-166.
[2] E.C. Le Ru, P.G. Etchegoin, Principles of Surface-enhanced Raman spectroscopy and related plasmonic effects, Elsevier, Amsterdam, 2009.
[3] M.D. Doherty, A. Murphy, J. McPhillips, R.J. Pollard, P. Dawson, J. Phys. Chem. C 114 (2010) 19913-19919.
[4] A.D. McFarland, M.A. Young, J.A. Dieringer, R.P. Van Duyne, J. Phys. Chem. B 109 (2005) 11279-11285.
[5] K. Kneipp, M. Moskovits, H. Kneipp (Eds.) Surface-enhanced Raman scattering: physics and applications, Topics Appl. Phys. 103, Springer-Verlag, Berlin Heidelberg, 2006.
[6] B. Vlčková, P. Matějka, J. Šimonová, K. Čermáková, P. Pančoška, V. Baumruk, J. Phys. Chem. 97 (1993) 9719-9729.
[7] M. Procházka, P. Mojzeš, B. Vlčková, P.-Y. Turpin, J. Phys. Chem. B 101 (1997) 3161-3167.
[8] J. Hanzlíková, M. Procházka, J. Štěpánek, J. Bok, V. Baumruk, P. Anzenbacher Jr., J. Raman Spectrosc. 29 (1998) 575-584.
[9] M. Procházka, J. Štěpánek, P.-Y. Turpin, J. Bok, J. Phys. Chem. B 106 (2002) 1543-1549.
[10] M. Procházka, P.-Y. Turpin, J. Štěpánek, B. Vlčková, J. Raman Spectrosc. 33 (2002) 758-760 and Langmuir 21 (2005) 2956-2962.
[11] M. Procházka, N. Hajduková, J. Štěpánek, Biopolymers 82 (2006) 390-393.
[12] N. Hajduková, M. Procházka, P. Molnár, J. Štěpánek, Vib. Spectrosc. 48 (2008) 142-147.
[13] P. Šimáková, M. Procházka, J. Mol. Struct. 993 (2011) 425-427.
[14] K. Kadish, K.M. Smith, R. Guilard (Eds.) Handbook of porphyrin science: with applications to chemistry, physics, materials science, engineering, biology and medicine, World Scientific Publishing, Singapore, 2010.
[15] R.G. Freeman, K.C. Grabar, K.J. Allison, R.M. Bright, J.A. Davis, A.P. Guthrie, M.B. Hommer, M.A. Jackson, P.C. Smith, D.G. Walter, M.J. Natan, Science 267 (1995) 1629-1632.
[16] C.D. Keating, M.D. Musick, M.H. Keefe, M.J. Natan, J. Chem. Educ. 76 (1999) 949-955.
[17] N. Hajduková, M. Procházka, J. Štěpánek, M. Špírková, Colloid Surf. A-Physicochem. Eng. Asp. 301 (2007) 264-270.
[18] N. Blom, J. Odo, K. Nakamoto, D. Strommen, J. Phys. Chem. 90 (1986) 2847-2852.
[19] P. Stein, A. Ulman, T.G. Spiro, J. Phys. Chem. 88 (1984) 369- 374.
[20] O.K. Song, M.J. Yoon, D. Kim, J. Raman Spectrosc. 20 (1989) 739-743.
[21] J. Qu, D.P. Arnold, P.M. Fredericks, J. Raman Spectrosc. 31 (2000) 469-473.
[22] J. Chowdhury, M. Ghosh, P. Pal, T.N. Misra, J. Colloid Interf. Sci. 263 (2003) 318-326.
[23] V. Thomsen, D. Schatzlein, D. Mercuro, Spectroscopy 18 (2003) 112-114.